

## Airborne Detection of Perfect Conductors: Project Gemini

Macnae, J. <sup>[1]</sup>, Smiarowski, A. <sup>[2]</sup>

1. School of Applied Sciences, RMIT University

2. Dept. of Physics, University of Toronto

### ABSTRACT

*High-grade nickel and copper sulphides appear as 'perfect conductors' to most electromagnetic and airborne electromagnetic systems, since they have bulk electrical conductivities of the order of 100,000 S/m. Their EM response is essentially undetectable with off-time measurements or when using non-rigid towed-bird systems. Compact AEM systems with accurate primary field bucking and on-time or in-phase measurements are sensitive to perfect conductors, but are incapable of detecting deep targets. Calculations in 2004 suggested that it should be easy for AEM to detect 'perfect conductors' using GPS systems to define geometry, provided the receiver was several hundred metres distant from the transmitter. A twin (Gemini) aircraft test was undertaken to test this concept in 2005. The field test was completely successful. Geometric and signal noise levels in the test were much better than 0.5% of the primary field at 400 m separation, allowing detection and characterisation of the 30Hz, in-phase response of both small and extended 'perfect conductors'. It is predicted that a 200 m by 100 m perfect conductor target should be detectable to depths of 200 m below surface using off-the-shelf technology.*

### INTRODUCTION

While airborne EM (AEM) has historically been quite successful in locating base metal and nickel deposits, analysis has shown that the economic 'cores' of many deposits are undetectable. This is because they have measured hand-specimen and bulk conductivities around 100,000 S/m (Emerson et al., 2001 & 2002), with corresponding skin depths of 50 cm if excited by a plane wave at a frequency of 10 Hz and a skin depth of only 16 cm at 100 Hz. These skin-depths are much less than typical deposit thickness and imply that AEM signals do not penetrate these deposits. This observation further suggests that the historic success of AEM was somewhat serendipitous in that the systems were most likely detecting the lower grade or non-economic haloes of economic deposits.

Predicted EM time constants using the standard tabular body formula and measured conductivities (Emerson et al., 2001, 2002) are in the vicinity of:

10MT Massive Nickel Sulphides	300 secs (5 minutes)
10MT Massive Copper Sulphides	4 secs
100MT Massive PbZn Sulphides	18 secs

These slow decays are out of the time range measured in the off-time by existing AEM systems. At the instigation of Ken Witherly, Macnae examined in late 2003 the issue of the airborne detection of 'perfect conductors' and concluded that a twinned aircraft or 'Gemini' system with geometry accurately

measured with GPS was likely to work. Three companies subsequently funded a modeling and feasibility study, namely Inco, Noranda-Falconbridge and BHP-Billiton. The feasibility research took place in 2004.

### Fundamental constraint for perfect conductor detection

Perfect conductors act as 'mirrors' to EM fields, and as such perfectly reflect any EM signals in their vicinity. Unlike other conductors where secondary responses can be seen decaying after excitation, isolated perfect conductor responses are only detectable through measuring distortions to the total field measured while the primary field is being transmitted (Grant and West, 1965). Perfect conductors in the vicinity of other conductors (including conductive host and cover) modify the other conductor's secondary response, but respond only while the other conductor has a secondary response. This tertiary effect of a perfect conductor will not be analysed in this paper, and we will focus on the isolated perfect conductor in a resistive host.

### Relative and Absolute response

The magnetic components of an EM field consist of the vector sum of a secondary field and a primary field. To estimate the secondary field there are two fundamental requirements: 1)

After all processes for noise reduction have taken place, the absolute residual secondary response must exceed the absolute residual ‘noise level’. 2) The relative amplitude of the secondary signal must exceed any uncertainty in the primary subtraction, whether through calculation or bucking.

In an AEM measurement there are many sources of electromagnetic noise: 1) Noise that affects the absolute ‘noise level’ includes spherics, microphonics (or rotation in the earth’s field), cultural, sensor and instrument, all of which are minimized by stacking and processing. 2) Noise that affects primary subtraction includes transmitter current stability and system geometrical uncertainty (of the transmitter, receiver and bucking systems).

**PROJECT AIMS**

The first aim of the feasibility study was to investigate the viability of an AEM system with a receiver in a separate aircraft from the transmitter (Figure 1). Such a system in fact flew in the 1950’s (Tornqvist, 1959, Fountain, 1998). The second aim was to devise a method to measure (or control) Tx-Rx geometry sufficiently accurately that residual secondary fields resulting from a perfect conductor may be measured in the presence of the primary field.

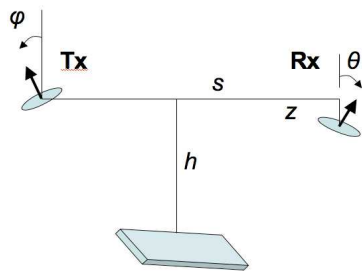


**Figure 1:** The Gemini concept. A transmitter Tx and receiver Rx with vertical offset z are located distance s apart, with rotations  $\phi$ ,  $\theta$  as shown. The system flies at height h above a perfectly conducting target.

**Absolute Response**

A total of 12000 inductive limit forward models were calculated with a coplanar Tx-Rx for conductors of varied strike length, dip, depth and transmitter-receiver distance (coil-separation), using code based on program MultiLoop. Figure 2 shows that the absolute peak response from a shallow-dipping target falls off as a function of both depth to target and coil separation.

Generally, it can be stated that for a vertical dipole transmitter and a vertical dipole receiver, the maximum absolute secondary response always occurs when they are coincident. For a small steeply-dipping target there is an additional coupling maximum, but space prevents further discussion of this case. Figure 2 amplitude scales are normalized to the primary field expected from a dipole transmitter of 1 million Am<sup>2</sup> as measured at a distance of 100 m. At this scale, the published noise levels (Smith 2001) for calculated B field Geotem data are shown in pink.

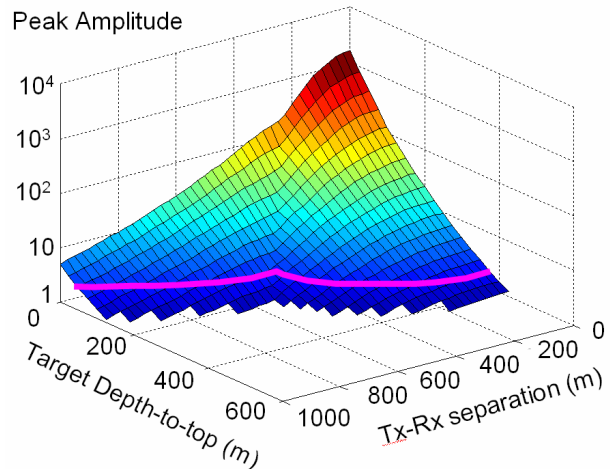


**Figure 2:** Normalised (absolute) peak amplitude of a 200\*150 m target, dip 30°, plotted as a function of target depth and transmitter-receiver separation. The pink line is equivalent to the Geotem B field noise level assuming a transmitter dipole moment of 1 million Am<sup>2</sup>

**Relative Response**

Since it is necessary to subtract a calculated primary from the measurement, it is quite instructive to determine the ratio of secondary to primary fields, particularly to determine where the ratio of secondary to primary is a maximum. This ratio is presented in Figure 3, corresponding to the shallowly dipping small target shown in Figure 2.

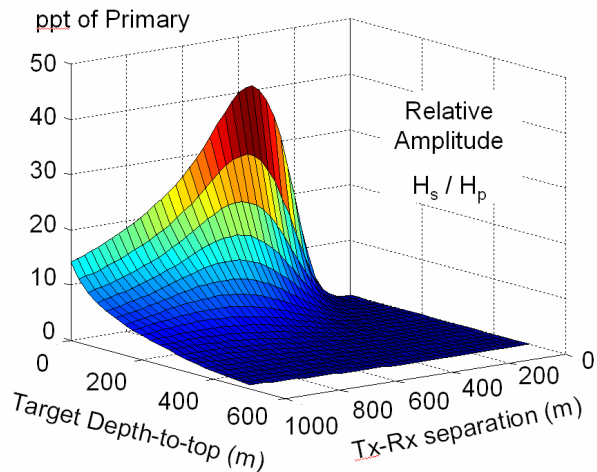


**Figure 3:** Ratio in parts per thousand of secondary to primary fields for the 200\*150 m target, dip 30°.

For this small target (Figure 3), the relative secondary field peaks at 40 ppt of the primary field at a coil separation around 400 m. With separations less than this, the receiver is much closer to the transmitter than the target, so the ratio drops. At large separations it is not possible to simultaneously get good coupling of both transmitter and receiver to the target.

Figure 4 presents an analysis of the required geometrical accuracy to achieve primary subtraction accurate enough for target detection, as a function of target depth and coil separation. Shown is the analysis for a coplanar system, basically an airborne Slingram geometry. At the typical fixed-wing separations around 100 m, accuracies in the cm range are required, consistent with Hefford et al., 2006. However, at 400 m separation, 1 m of relative geometrical error would be adequate for primary field calculation even with depths of up to 300 m for the small target. The conclusions were to use off-the-shelf GPS navigation systems to provide the required geometrical accuracy for primary calculation and subtraction.

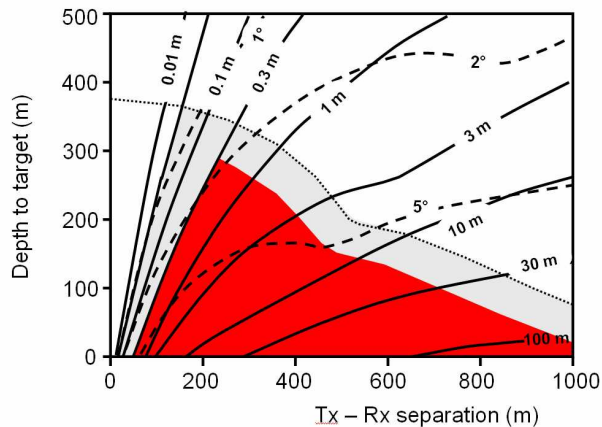


**Figure 4:** Contours of permitted distance error in m and permitted Tx rotation error in degrees as a function of retransmitter-receiver separation and depth-to-top of the 200\*150 m, 30° dip target. The contour values correspond to the distance or orientation error equivalent to the peak target response. The area shaded red would be clearly detectable using a good coil sensor and GPS navigation, with the area in grey marginal. The dotted line above the grey area corresponds to published Geotem B field noise levels.

### THE FIELD TEST

On October 17, 2005, the first field test of the Gemini concept was conducted over three test areas, funded by Spectrem Air and the three original sponsors. We will present data from two of these areas, one containing a small target and the other a set of extended conductors. Briefly, the 3 component AFMAG sensor of Geotech (for description, see Lo 2004) was operated beneath a helicopter at a nominal distance of 400 m behind an operating VTEM transmitter. Helicopter separation was maintained visually, with operator feedback using the observed primary field amplitude. High-end GPS systems were attached to both the AFMAG receiver shell and at 6 points around the VTEM transmitter loop, allowing accurate monitoring of their relative positions at 0.2 second intervals. Accuracy in relative positions was statistically estimated to be better than 2 cm horizontal and 10 cm vertical.

Using the monitored loop and receiver locations, the expected primary field of the VTEM transmitter at the receiver was accurately calculated, taking into account the transmitter loop attitude, location and distortion. From 3 component

AFMAG data, continuously sampled at 2000 Hz, the data was binned into 0.2 second windows, each consisting of 400 samples in 3 components. The in-phase and quadrature amplitudes of the observed signal transmitted by the 30Hz VTEM system were calculated, allowing for asynchronicity of the VTEM and AFMAG system clocks. After determination of scaling factor, the difference between the observed and calculated fields is the Gemini response which is similar in anomaly shape and interpretation to the ground Slingram system response.

The system was operated at high-altitude to determine noise levels, which were determined to be a strong function of the ubiquitous 60Hz noise detected throughout the survey region. Away from the major powerlines however, Gemini response noise levels achieved were significantly better than 1% of the primary field. High spatial frequency noise of amplitude about 0.2% is attributed to powerline noise, sensitivity limit, timing jitter between 16 bit AFMAG data acquisition system and the asynchronous VTEM transmitter. Low spatial frequency responses are attributed to current drift and/or GPS systematic errors.

### Small target

The line over the centre of the small target was flown at 3 different altitudes: 1) 'straight and level' at a nominal Tx and Rx altitude of 150 m; 2) 'straight and level' at a nominal Tx and Rx altitude of 100 m; and 3) in draped flight as if on a normal survey. After extensive processing of this data, we obtained the 30 Hz inphase responses as shown as solid lines in Figure 5. The processing included: 50 Hz, sferic and microphonic background removal from the 3 component AFMAG time series; constrained resampling of asynchronous data to achieve synchronous amplitude and phase detection, primary field calculation and normalisation to present the total observed secondary as a fraction of the primary.

With significant topography on the survey line, altitude and separation varied considerably along each of the overflights. Altitude and separation control were determined by pilots with regard to safety, radar altimeter readings and verbal "too close" or "too far" directions by the operator of the AFMAG system who was monitoring the 30Hz VTEM signal strength. A survey aim was to keep separation close to 400m. In fact, separations varied from 330m to 540 m during the three passes over the target.

Preliminary Maxwell modelling of the data was undertaken to assess the responses detected. Three straight lines at different altitudes with a constant 400 m Tx-Rx separation were used to approximate the survey geometry. Using externally provided data to fix the target size at 100 by 150 m, the dip and depth below surface were changed until a simultaneous fit to the observed data at the three altitudes was achieved. While the Maxwell model shown in Figure 6 is a reasonably good approximation of the data, in practice the separation and altitude was quite variable along the survey line. Proper interpretation would require modelling of the actual flight path and Tx-Rx separation, as well as geometry including use of the 3 receiver components measured. This modelling has not been attempted prior to this report. With the noise levels achieved, this small

target could be detected up to a depth of about 150 m (in a resistive host).

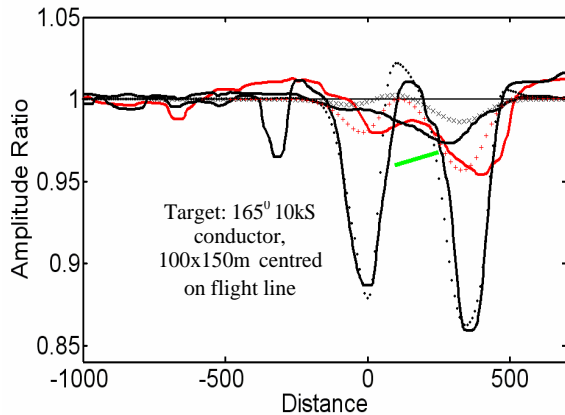


**Figure 5:** The Gemini results at the three different survey altitudes with solid lines, altitude 40m and 140 m (black), 90m (red), plotted as a fraction of the calculated primary field. Clear is a negative response in the form of a 400 m wide dual trough at the lowest altitude. Maxwell modelling results for a Tx-Rx separation of 400m are shown by dots, crosses and x's for 40m, 90m, and 140m altitude, respectively.

Calculated inphase and quadrature data at the first and third harmonics of the VTEM waveform are shown in Figure 6. It is clear that the in phase data shows a much more pronounced anomaly at the target than quadrature data. The quadrature data show some drift and background variations.

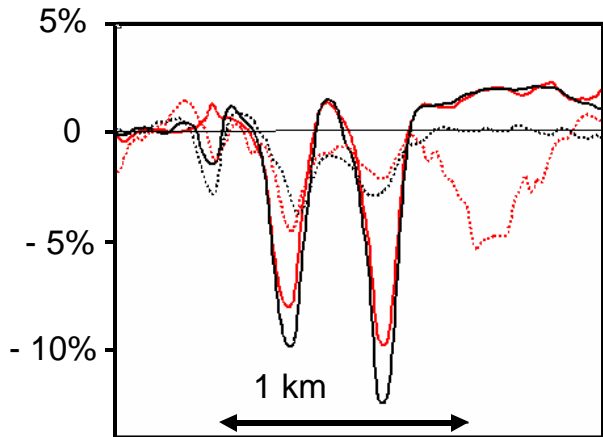


**Figure 6:** The calculated 30 (red) and 90 Hz (black) responses over the small target; inphase solid, quadrature dotted.

**Extended target**

The line over three extended targets is shown in Figure 7. The response shows large positives in the in-phase, typical of layered earth responses in an elevated Slingram configuration. Conductivities estimated using a half-space model vary along the line, with about 150 mS/m as the typical background. Three steeply-dipping conductors are detected within this background

at locations C1, C2 and C3. The most conductive of these is C1, calculated to show conductivity of > 10 S/m, and which is attributed to a particularly conductive graphite body.

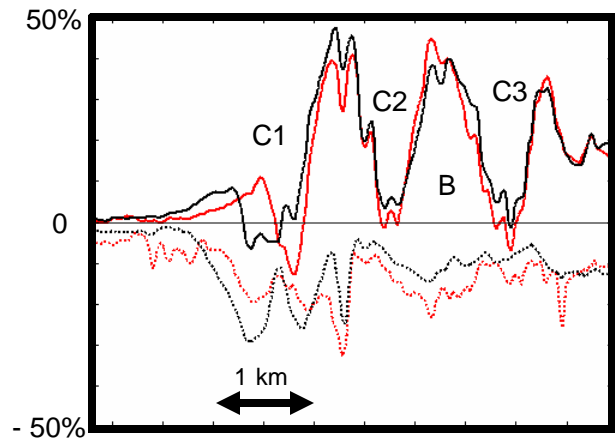


**Figure 7:** The fundamental 30 (red) and third harmonic 90 Hz (black) responses over the extended targets. Solid inphase and dotted quadrature responses at B correspond to 150 mS/m. High apparent conductivity (> 10000 mS/m) at target C1 has caused the 30 and 90 Hz inphase responses to be significantly displaced from each other, with 1200 mS/m estimated at targets C2 and C3.

**CONCLUSIONS**

The study here investigates geometrical constraints and required noise levels for detection of a large inductive limit target. The analysis of a Gemini-type configuration led to a field test using a 400 m TX-RX separation. Signal noise levels were much better than 0.5% of the primary field using a nominal flight separation of 400m. The test over a small, shallow conductor was successful, and suggests perfect conductors can be detected by a Gemini system to considerable depths.

**ACKNOWLEDGEMENTS**

We thank Condor Consulting, RMIT University, sponsors BHP Billiton and Spectrem Air, and the former Falconbridge and Inco for support for this project, as well as Tim Dohey and Aaron Davis for field and processing contributions.

**REFERENCES**

Emerson, D. W., Williams, P.K., and Luitjens, S., 2001., The conductivities of Komatiitic nickel ores at Kambalda, WA, ASEG Preview 92, 38-41

Emerson, D. W., Fallon, G. N. and Fullagar, P. K., 2002, Physical properties of zinc and iron rich volcanogenic massive sulphides: laboratory scale measurements results, ASEG Preview 96, 16-20.

Fountain, D., 1998, Airborne Electromagnetic systems – 50 years of development. Exploration Geophysics 29, 1-11.

Grant, F.S. and West, G.F., 1965, Interpretation Theory in Applied Geophysics, McGraw-Hill Book Company.

Hefford, S. W., Smith, R. S. and Samson, C., 2006, Quantifying the Effects That Changes in Transmitter-Receiver Geometry Have on the Capability of an Airborne Electromagnetic Survey System to Detect Good Conductors, Exploration and Mining Geology 15., 43-52.

Lo, R. and Kuzmin, P., 2004, AFMAG: Geotech's New Airborne Audio Frequency Electromagnetic (EM) System, Houston Geological Society 47, November.

Smith, R. S., 2001, On removing the primary field from fixed-wing time-domain airborne electromagnetic data: some consequences for quantitative modelling, estimating bird position and detecting perfect conductors. Geophysical Prospecting. 49, 112-126.

Tornqvist, G., 1959, Some Practical Results of Airborne Electromagnetic Prospecting in Sweden, Geophysical Prospecting, 6, 112-126.